0.09 mg Lysozyme in 30 mg PLGA, TOO LOW Concentration

European Journal of Pharmaceutics and Biopharmaceutics 82 (2012) 498–507

Contents lists available at SciVerse ScienceDirect

European Journal of Pharmaceutics and Biopharmaceutics

journal homepage: www.elsevier.com/locate/ejpb

Research paper

Preparation of polymeric particles in CO_2 medium using non-toxic solvents: Formulation and comparisons with a phase separation method

My-Kien Tran, Amin Swed, Frank Boury *

LUNAM Université, Angers, France
INSERM U1066, Micro et Nanomedécines Biomimétiques, IBS, Angers Cedex 9, France

ARTICLE INFO

Article history:
Received 2 April 2012
Accepted in revised form 20 August 2012
Available online 29 August 2012

Keywords:
Non-toxic solvents
Protein encapsulation
Drug delivery systems
Experimental design
CO_2
Poly-lactic-co-glycolic acid (PLGA)

ABSTRACT

The aim of this work was to elaborate formulation strategies to encapsulate a protein into biodegradable polymeric particles for sustained release purpose. In this paper, two encapsulation methods will be presented, one dealing with a phase separation phenomenon while the other involving an emulsification/extraction process in CO_2 medium. In those methods, only non-volatile injectable solvents such as glycofurol or isosorbide dimethyl ether were used to dissolve the polymer. Moreover, experimental designs were built up to help us to go further in the understanding of the processes and to better predict output responses in design space. Spherical particles were successfully generated with a satisfactory encapsulation yield. Further characterization steps such as *in vitro*, *in vivo* releases will be carried out to validate the interest of our encapsulation methods in the development of drug delivery systems.

1. Introduction

Protein encapsulation in biodegradable polymers has been drawing attention of researchers since decades [1,2], and it is still the subject of many publications in recent years [3,4]. This research topic arises from the fact that many therapeutic proteins have been discovered and the encapsulation of these molecules into a controlled release system can improve the therapeutic efficiency and offers benefits to patient comfort [5]. Hence, many encapsulation methods have been developed to respond to the actual need such as: water/oil/water (w/o/w) [6], solid/oil/water (s/o/w) [7], simple coacervation [8], and other derivative methods [9,10]. Although each method presents its own disadvantages, proteins can be encapsulated more or less successfully by these methods. With no intention to be exhaustive, some disadvantages of each method are listed below for illustration purpose. For instances, in the w/o/w method, proteins may absorb at w/o interfaces, unfold, and loss their integrity [5]. To avoid destructive w/o interfaces, s/o/w and solid/oil/oil (s/o/o) have been developed and their utility has been proven by many works [3,7,11,12]. However, amount of residual solvent and nonpolar character of the continuous phase are considered as drawbacks in s/o/o method while low encapsulation efficiency and the diffusion of stabilizing agents into the water phase are issues of s/o/w method [13]. In classic simple coacervation method, which was widely used for protein and peptide encapsulation, the main problem lies in the toxicity of residual coacervating and hardening agents remaining in the final product [14].

In those methods mentioned above, the use of volatile solvents such as halogenated solvents is rarely avoided, which is harmful to human health and the environment. Hence, it is of great importance to find ways of avoiding the use of these solvents in the encapsulation process. An interesting approach was developed based on the PGSS (Particle Gas Saturated System) method, which allows poly-lactic-co-glycolic acid (PLGA) microparticles to be formed in CO_2 medium without using any organic solvent in a mild condition of temperature [15]. Moreover, it was reported that there was no significant loss of activity of proteins encapsulated by this technique. However, according to the authors, it is difficult to control the size, shape, and drug release kinetics of this type of PLGA microparticles [15]. Therefore, this technique requires further improvements to prove its interest in the development of protein delivery system. Another approach is to use non-volatile water-miscible solvents [16,17], which are much safer than the volatile ones. One example of this approach is the work of Bilati et al. [18] in which DMSO or *n*-methyl pyrrolidone was used to dissolve PLGA and proteins. PLGA nanoparticles were formed by a process called nanoprecipitation when polymer solution was put in contact with a non-solvent of PLGA like water or ethanol.

In this paper, we present two encapsulation methods where protein was firstly precipitated and the suspension of protein precipitates was then mixed with a polymer solution prepared in

* Corresponding author. INSERM U1066, Micro et Nanomedécines Biomimétiques, IBS, 4 rue Larrey, F-49933 Angers Cedex 9, France. Tel.: +33 2 44 68 85 28; fax: +33 2 44 68 85 46.
E-mail address: frank.boury@univ-angers.fr (F. Boury).

0939-6411/$ - see front matter © 2012 Elsevier B.V. All rights reserved.
http://dx.doi.org/10.1016/j.ejpb.2012.08.005

glycofurol (GF) or in a mixture of GF and isosorbide dimethyl ether (DMI). To our best knowledge, GF and DMI are the two safest injectable solvents used in different drug products for parenteral or other therapeutic uses [19–24] with a consistently low toxicity demonstrated through many studies [24–27]. This is the rationale of our work on the formulation of PLGA particles using different preparation methods. In this present paper, as our first piece of work related to protein encapsulation in PLGA particles using water-miscible injectable solvents, two encapsulation methods named emulsification/extraction method in CO_2 medium and phase separation method will be shown. The aim of this work was to optimize these two encapsulation processes using experimental design. Different formulation variables such as solvent composition, pH, and polymer concentration were studied to allow optimal conditions of encapsulation process to be found. Besides, comparisons between these two processes will be made.

2. Materials and methods

2.1. Materials

Lysozyme (chicken egg-white), *Micrococcus lysodeikticus*, glycofurol (tetraglycol or α-[(tetrahydro-2-furanyl) methyl]-ω-hydroxy-poly(oxy-1,2-ethandiyl), and isosorbide dimethyl ether (1,4:3,6-Dianhydro-2,5-di-O-methyl-D-glucitol) were obtained from Sigma–Aldrich (Saint Quentin Fallavier, France). Uncapped 75/25 PLGA provided by Phusis (Saint-Ismier, France) had a mean molecular weight of 21,000 Da (polydispersity index $I = 1.8$) as determined by size-exclusion chromatography (standard: polystyrene). Poly (ε-caprolactone) (Capa® 6250, *Mw* 25,000) was kindly supplied by Perstorp (Warrington, England). Lutrol F68 and Lutrol F127 were purchased from BASF (Laserson, France).

2.2. Methods

2.2.1. Preparation of particles using phase separation method

2.2.1.1. Preparation of protein precipitates. Protein precipitation using GF had been optimized by Giteau et al. [28]. Precipitation condition of experiment number 4, which is one of the optima found by the author, was chosen to perform the precipitation step. Concretely, lysozyme was dissolved in 0.16 M NaCl solution at the concentration of 20 mg/ml. Thereafter, 25 µl of this solution was then mixed into 975 µl of glycofurol, which played here a role of anti-solvent, to obtain a suspension of precipitated protein for further use.

2.2.1.2. Preparation of polymer solution. A stock solution of 12% (w/v) PLGA in glycofurol was firstly prepared. Concentrations in this present paper will be expressed in w/v unless otherwise stated. Precisely, after adding PLGA to glycofurol, the mixture was left under stirring for about 48 h and then was left to stand for at least 7 days at room temperature. During this period of time, a macroscopic evolution of polymer solution was observed. This phenomenon was probably due to a reorganization of polymer chains with time leading to a partial precipitation of polymer from the solution. Before any further use, the solution was filtered through 0.2 µm pore size filter (Minisart RC 25, Sartorius Stedim).

2.2.1.3. Preparation of protein-loading particles. Firstly, 100 µl of suspension of protein precipitates in GF was added into 200 µl of polymer solution in GF to obtain finally a suspension of protein precipitates in polymer solution. The final polymer concentration in this suspension was either 5% or 8%. A certain amount of ethanol (50–150 µl) was then added into it, right before some volume (0.9–1.8 ml) of a 1% Lutrol F68 solution (solution X) was added into this mixture to start the phase separation. Thereafter, 15 ml of a 1% Lutrol solution in glycin buffer 1.25 mM pH (9–11) (solution Y) was introduced into the suspension. pH was measured using a MicropH2001pH-meter with a resolution of 0.01 pH (Crison Instruments, Paris, France). It should be noted that pH below 9 did not give a good result in terms of particle collection after centrifugation based on our previous work. After 15 min, 15–25 ml of the solution Y was added into the suspension and this suspension was left to stand for 12–24 h for the extraction step. It should be noted that at the end of the formulation, pH was found to be around 7. After that, the suspension of particles was concentrated by successively centrifuging at 1000*g* for 30 min and then 2000*g* for 30 min. Only redispersible particles were collected and the supernatant was eliminated. The final volume of the suspension was about 1 ml. This suspension was then freeze-dried for further quantification. A brief procedure is summarized in Fig. 1.

To optimize the formulation procedure, an experimental design was used. At the outset of our experimental program, a screening design was carried out to evaluate the impact of different operating factors. Seven following factors were chosen to be studied: *A* (extraction time), *B* (pH of solution Y), *C* (total volume of the suspension), *D* (volume ratio between polymer solution and solution X), *E* (ethanol volume), *F* (extraction temperature), and *G* (polymer concentration). In this set of experiments, a two-level saturated fractional factorial design 2^{7-4}_{III} was used to get insight into the possible significant effects. Factorial effects defining contrast are $I = ABD = ACE = AFG = BCF = BEG = CDG = DEF = ABCG = ABEF = ACDF = ADEG = BCDE = BDFG = CEFG = ABCDEFG$. With this type of low-resolution design, main effects are confounded with two-factor interaction (2FI) effects. In fact, on the assumption that third order (3FI) effects are not significant, in our case of seven factors, main effects will be aliased with two-factor interactions as follows [29]:

$$[A] = A + BD + CE + FG$$
$$[B] = B + AD + CF + EG$$
$$[C] = C + AE + BF + DG$$
$$[D] = D + AB + CG + EF$$
$$[E] = E + AC + BG + DF$$
$$[F] = F + AG + BC + DE$$
$$[G] = G + AF + BE + CD$$

Therefore, a foldover (mirror-image fold-over) design was applied in order to free the main effects from two-factor interactions [29,30]. After knowing the active factors, response surface methodology may be used to optimize the process. Design-Expert® 8

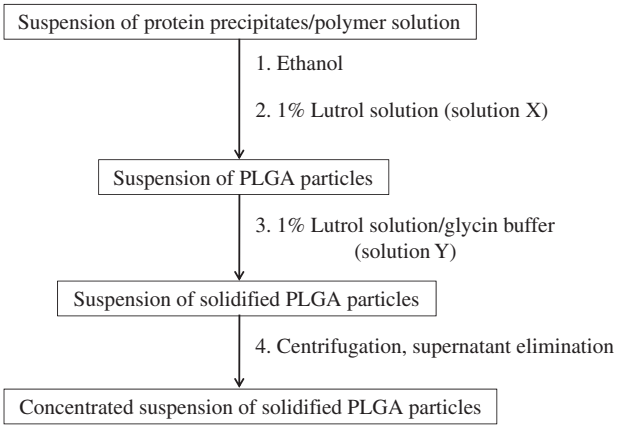

Fig. 1. Flow chart of the procedure used for the preparation of protein-loading PLGA particles by phase separation.

(Stat-Ease, Minneapolis, US) package was used for experimental design and data analysis.

2.2.2. Preparation of particles using emulsification/extraction method in CO_2 medium

2.2.2.1. Preparation of protein precipitates. In this series of experiments in CO_2 medium, our goal was to study the influence of the composition of solvent mixture used to dissolve polymer on the encapsulation yield under fixed conditions of pressure and temperature. Due to the fact that PLGA is much more soluble in DMI than in GF, it was decided to prepare protein precipitates using DMI instead of using GF in order to minimize the time of homogenization when the suspension of protein precipitates was added into polymer solution.

Like in the case of GF, protein was firstly dissolved in a solution of NaCl. This solution was then mixed with DMI to allow protein precipitates to be formed. In order to optimize the precipitation condition, an experimental design was built up using a Doehlert matrix [31] in which ionic strength, volume of aqueous phase and protein quantity with the following characteristics were chosen to be studied as variables:

- *Ionic strength (X_1):* center point – 0.3 M; step size – 0.29 M.
- *Volume of the aqueous phase (X_2):* center point – 90 μl; step size – 75 μl.
- *Protein quantity (X_3):* center point – 0.9 mg; step size – 0.5 mg.

The final total volume after mixing the protein solution with DMI was 1 ml.

This approach was inspired by the previous work of Giteau et al. [28] except that the range of protein quantity was modified to suit our purpose. Lysozyme was chosen as protein model and activity yield of lysozyme precipitates was the output to be measured. It was determined by measuring the turbidity of *M. lysodeikticus* suspension at 450 nm after an appropriate dilution (cf. Section 2.2.3.2). A series of 13 distinct experiments uniformly distributed in the spherical domain (Fig. 2) was firstly carried out (Table 1). The center point of experimental domain was repeated six times to estimate the pure experimental error. The postulated empirical model used to calculate the response from the input variables was as follows:

$$Y = \beta_0 + \beta_1 X_1 + \beta_2 X_2 + \beta_3 X_3 + \beta_{12} X_1 X_2 + \beta_{13} X_1 X_3 + \beta_{23} X_2 X_3 + \beta_{11} X_1^2 + \beta_{22} X_2^2 + \beta_{33} X_3^2 + \beta_{123} X_1 X_2 X_3$$

In order to validate the postulated model, four check points uniformly distributed in the design space were added to the previous set of experiments. Their distance from the center point is half the radius of the chosen spherical domain. At these check points, the differences between the actual yields obtained through observation and those obtained through theoretical calculation from the empirical model were then compared with the experimental error. Besides, an ANOVA analysis was performed to test the significance of the chosen model and the overall lack-of-fit of the experimental points in the domain. Nemrodw® (LPRAI, Marseille, France) was used for experimental design and data analysis.

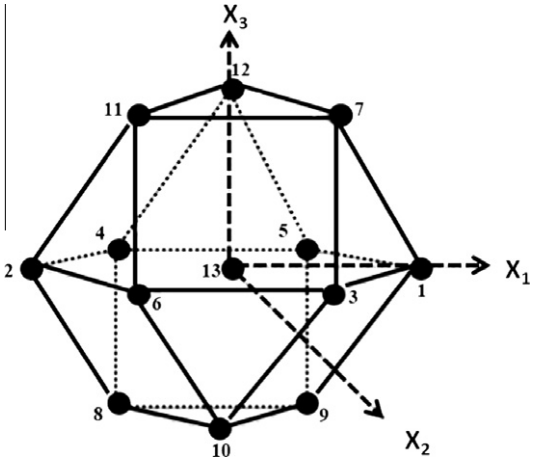

Fig. 2. Distribution of experimental points in design space (Doehlert matrix).

2.2.2.2. Preparation of protein-loading particles. The following preparation procedure was adapted from a process patented by our laboratory [32]. A scheme of the experimental setup used for the preparation of PLGA particles is shown in Fig. 3. Firstly, 0.4 ml of a suspension of lysozyme precipitates in polymer solution was introduced in a 14 ml view-cell (E1), which was kept at the operating temperature (39.6 ± 0.1 °C) by a thermostated water bath. Lysozyme and PLGA amounts were, respectively, 0.09 mg and 30 mg. The suspension was prepared by adding 100 μl of lysozyme precipitates in DMI with 300 μl polymer solution. CO_2 was then delivered to the cell by means of a membrane pump. The mechanical stirring was kept at 1500 rpm to favor the formation of an emulsion in CO_2. Once the desired pressure (80 ± 0.1 bars) was reached, 1.5 ml of 1% Lutrol F68 solution prepared in glycin buffer (0.625 M) pH 10 (E2) was injected to the cell using a HPLC pump. The stirring was kept for 20 min before a depressurizing step. A suspension of particles was then collected in (E3), which contained 5 ml of 9% Lutrol F127 solution (solution E4). This suspension was left to stand for 30 min before 35 ml of solution E4 was added into it. This final suspension was left to stand at ambient temperature (≈25 °C) for 8 h. Thereafter, the suspension was centrifuged at 2000*g* for 30 min, which allows particles to be collected. Particles were washed one time with distilled water before being freeze-dried.

We believe that under known conditions of temperature and pressure, emulsification in CO_2 medium and the consequent impact on the encapsulation yield will strongly depend on the composition of solvent mixture. Hence, a mixture design was built up in which DMI, GF, and ethanol were chosen as components and Scheffé canonical polynomials [33] were chosen as regression models. These three components vary as shown:

$$0.25 \leqslant A \text{ (DMI)}$$
$$0 \leqslant B \text{ (GF)} \leqslant 0.5$$
$$0 \leqslant C \text{ (ethanol)} \leqslant 0.25$$
$$A + B + C = 1$$

The total volume of solvents and the amount of PLGA were respectively fixed at 400 μl and 30 mg. 100 μl of protein suspension, which was used to mix with 300 μl of polymer solution, was considered as 100 μl of DMI in the calculation of solvent composition.

The experimental domain with the chosen constraints is not a simplex. Thus, point exchange algorithm and coordinate exchange algorithm [34] have been used to search experimental points across the design space based on IV-optimum (I-optimum) criterion, which minimizes the integral of prediction variance over the experimental domain [35]. Quadratic model was firstly chosen for our study. A series of 11 distinct experimental points was then found based on the above-mentioned criterion. Some points were repeated for the estimation of the pure experimental error (five degrees of freedom). The model may be eventually augmented if necessary by adding extra points to the design space. Design-Expert® 8 (Stat-Ease, Minneapolis, US) package was used for experimental design and data analysis.

Table 1
Experimental points with the corresponding activity yield of protein precipitates prepared using DMI.

No. exp.	Ionic strength (M)	Aqueous volume (μl)	Protein quantity (mg)	Activity yield (%)
1	0.59 (1.000)	90.0 (0.000)	0.9 (0.000)	90.6
2	0.01 (−1.000)	90.0 (0.000)	0.9 (0.000)	94.9
3	0.44 (0.500)	155.0 (0.866)	0.9 (0.000)	97.0
4	0.16 (−0.500)	25.0 (−0.866)	0.9 (0.000)	90.7
5	0.44 (0.500)	25.0 (0.866)	0.9 (0.000)	76.7
6	0.16 (−0.500)	155.0 (0.866)	0.9 (0.000)	90.9
7	0.44 (0.500)	111.7 (0.289)	1.3 (0.816)	81.5
8	0.16 (−0.500)	68.3 (−0.289)	0.5 (−0.816)	80.9
9	0.44 (0.500)	68.3 (−0.289)	0.5 (−0.816)	100.0
10	0.30 (0.000)	133.3 (0.577)	0.5 (−0.816)	100.0
11	0.16 (−0.500)	111.7 (0.289)	1.3 (0.816)	80.0
12	0.30 (0.000)	46.7 (0.577)	1.3 (0.816)	88.5
13	0.30 (0.000)	90.0 (0.000)	0.9 (0.000)	92.9
14	0.30 (0.000)	90.0 (0.000)	0.9 (0.000)	90.5
15	0.30 (0.000)	90.0 (0.000)	0.9 (0.000)	102.0
16	0.30 (0.000)	90.0 (0.000)	0.9 (0.000)	98.0
17	0.30 (0.000)	90.0 (0.000)	0.9 (0.000)	94.9
18	0.30 (0.000)	90.0 (0.000)	0.9 (0.000)	97.0
19	0.18 (−0.408)	72.3 (−0.236)	0.8 (−0.167)	87.5
20	0.42 (0.408)	72.3 (−0.236)	0.8 (−0.167)	90.0
21	0.30 (0.000)	125.4 (0.471)	0.8 (−0.167)	102.5
22	0.30 (0.000)	90.0 (0.000)	1.1 (0.500)	94.5

Values in parentheses are coordinates of experimental points presented in coded form.
Point numbers 19, 20, 21, and 22 were check points used for the validation of empirical model.

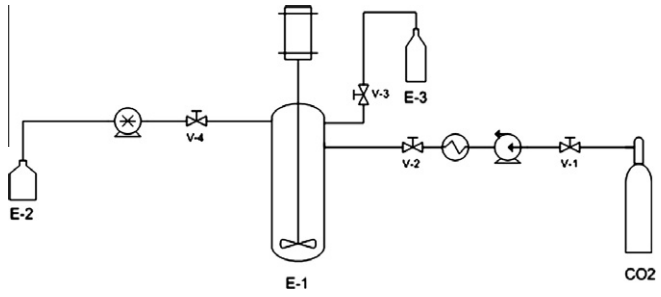

Fig. 3. Schematic diagram of the experimental setup.

2.2.3. Particles characterization

2.2.3.1. Morphology and size. The surface morphology of the particles was investigated by scanning electron microscopy (SEM) (JSM 6310F, JEOL, Paris, France) at accelerating potential of 3 kV. Freeze-dried particles were mounted onto metal stubs using double-sided adhesive tape and then vacuum-coated with a film of gold using a MED 020 (Bal-Tec, Balzers, Lichtenstein).

Particle size was determined by dynamic light scattering technique. A Nanosizer® (Malvern Instruments, Worcestershire, UK) was used in the case of particles prepared by phase separation while those obtained from emulsification/extraction method were measured by a Mastersizer® 2000HS (Malvern Instruments, Worcestershire, UK). Suspensions of particles in distilled water before freeze-dried step were used for these analyses.

2.2.3.2. Encapsulation yield of protein. The biologically active entrapped protein was determined using *M. lysodeikticus* [3,28]. Briefly, the total amount of each batch (15–30 mg according to experiment conditions) of freeze-dried lysozyme-loaded microparticles obtained after formulation was dissolved in 0.9 ml of DMSO. After 1 h, 3 ml of 0.01 M HCl was added. The solution was left to stand for 1 more hour and then diluted to an appropriate range of concentration before being incubated overnight with a suspension of *M. lysodeikticus*. Lysozyme activity determination was based on turbidity measurement at 450 nm (UVIKON 922, Kontron Instruments, France). The amount of encapsulated active protein was calculated using a standard curve after subtraction of the control value of blank sample. The blank sample was prepared in the same condition of protein-loaded sample in absence of protein precipitates. It should be pointed out that blank sample did not show any lysis effect on *M. lysodeikticus.*

2.2.3.3. DSC analysis. Differential scanning calorimetry (DSC) was performed with a Mettler Toledo Star System (Mettler-Toledo, Viroflay, France). Approximately, 10 mg of sample was placed in a sealed aluminum DSC pan without hole. The measurements were carried out at 5 °C min^{-1} under nitrogen flow. The sample was firstly heated to 70 °C. Thereafter, the sample was cooled down to 0 °C before being reheated to 70 °C. Thermal data were taken from the second heating step using the supplied software.

3. Results and discussions

3.1. Formulation of lysozyme-loading particles using phase separation method

At the initial stage of our experimental program, screening design was firstly performed to find influential factors on the encapsulation yield. It can be seen in the half-normal plot (Fig. 4) that only the estimation of the effect of factor *B* (pH) falls off to right of the line, which means this effect has contributed the most to the variation of the response. Other effects falling in line, which represents a normal scatter presumably due to experimental error, are probably insignificant. As already said in the method part, the factor *B* confounds with some of two-factor interactions such as *AD*, *CF*, and *EG*. In order to clear the factor *B* of these two-factor interactions and to be able to conclude whether factor pH is significant or not, the initial design was augmented by adding its mirror image to perform a foldover design. The result is shown in Fig. 5 and this time, factor *B* (pH) is confirmedly active.

At this stage of the work, our wish was to study the influence of pH on the response and eventually find the optimum condition for the encapsulation process. Hence, while keeping other factors constant, pH was gradually modified in the chosen range and then the consequent variation of the encapsulation yield was noted. It can

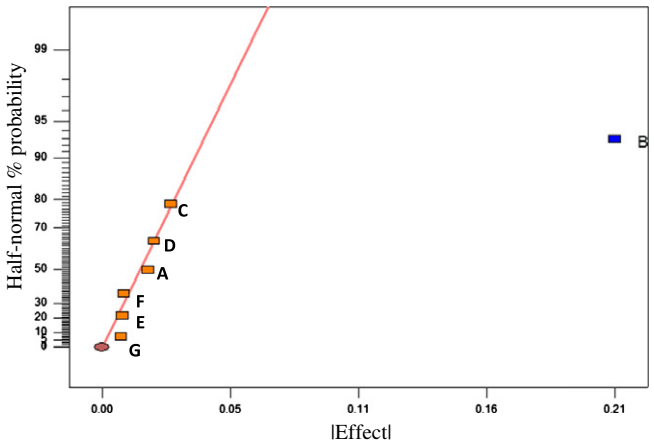

Fig. 4. Half-normal plot of effects for encapsulation yield. (For interpretation of the references to color in this figure legend, the reader is referred to the web version of this article.)

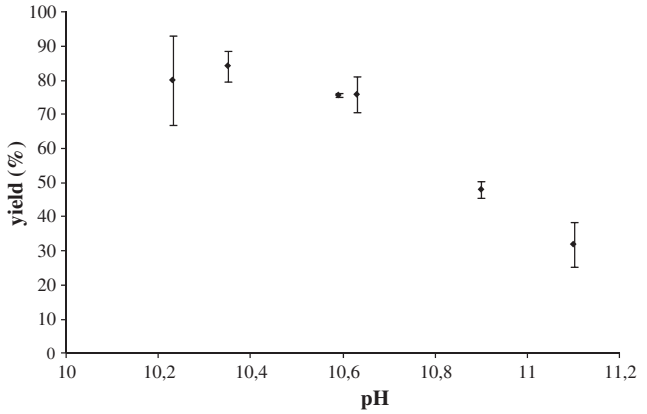

Fig. 6. Variation of encapsulation yield according to pH (error bars are presented as standard error of mean, $n = 3$).

be noted in Fig. 6 that encapsulation yield does not change much in a range of pH from 10.25 to 10.65. It can be found 75–85% of encapsulation yield in this range with a maximum of 85% at pH of 10.35. Outside this range, encapsulation yield begins to decrease, which is maybe a sign of the onset of PLGA hydrolysis in alkaline medium.

The size of particles in suspension form, determined by Nanosizer, is about 250 nm (Table 8), which is coherently confirmed by the observation of freeze-dried powder under electron microscopy (Fig. 11A). Freeze-dried particles appear to be spherical but aggregated. It suggests that there is residual GF still remaining in the particles ($T_g = 27.5$ °C compared to $T_g = 45$ °C of pure PLGA) [36]. However, obtaining a powder form is not our ultimate goal in this formulation part. At this stage, it seems fair for us to say that a suspension form of protein-encapsulated PLGA particles, which would be used for parenteral applications, is successfully formulated. Besides, it needs to be emphasized that the aim of this work is to encapsulate a therapeutic protein, which is generally very fragile and easily denatured by different factors. PLGA particles with a less pronounced aggregation can be seen in Fig. 11B. This batch of particles can be prepared by increasing ionic strength and buffer capacity of the solution Y, which is harmful for protein activity but might be useful, for instance, in the case of encapsulation of a lipophilic drug like many anti-cancer drugs. Indeed, PLGA particles with an average size of 250 nm prepared by this method may be suitable for a passive tumor targeting based on enhanced permeability and retention (EPR) effect. Although the optimal size for EPR effect has not been precisely determined yet, it can be found in the literature that the cutoff size of the pore in tumor vessels is between 400 and 600 nm suggested by a study using liposomes as carriers [37] or can be ranging from 200 nm to 2 μm based on a direct observation of tumor vasculature [38,39]. However, it should be noted that the pore size is tumor-dependent and the permeability can vary during tumor progression as well as the anatomical location [38,40].

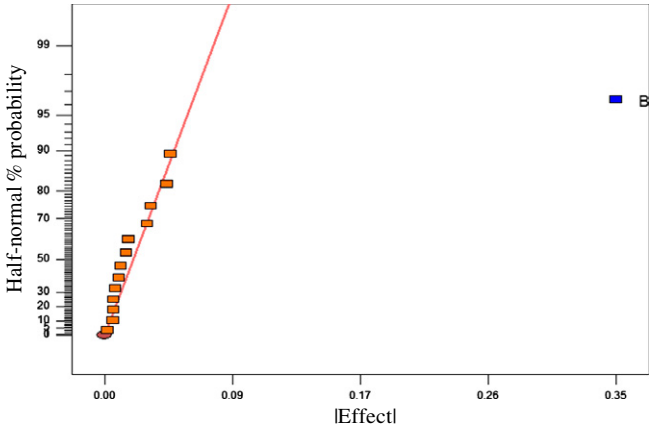

Fig. 5. Half-normal plot of effects for encapsulation yield of lysozyme after foldover (from left to right are the estimation of *E*, *BE*, *F*, *G*, *DE*, *D*, *DG*, *DF*, *CE*, *CF*, *C*, *EF*, *A*, *B*). (For interpretation of the references to color in this figure legend, the reader is referred to the web version of this article.)

3.1.1. Underlying mechanism of the encapsulation process

Since protein precipitates were prepared using precipitation process and were freshly mixed with polymer solution, we believe that protein precipitates were in solvated state and had a surrounding liquid surface of GF, which is the solvent of PLGA. Therefore, like in the case of classic simple coacervation method, the interfacial tensions between drug-phase and coacervate/continuous phases play the essential role in the final result [8]. Solvated protein precipitates, continuous phase (H_2O), and coacervate phase are denoted as L1, L2, and L3, respectively. A complete encapsulation occurs when the following conditions are satisfied:

$$S_1 = \gamma_{L2/L3} - (\gamma_{L1/L2} + \gamma_{L1/L3}) < 0$$
$$S_2 = \gamma_{L1/L3} - (\gamma_{L1/L2} + \gamma_{L2/L3}) < 0$$
$$S_3 = \gamma_{L1/L2} - (\gamma_{L1/L3} + \gamma_{L2/L3}) > 0$$

It can be seen that the lower $\gamma_{L1/L3}$'s value is, the lower S_2 is, the higher S_3 is, and thus the more L3 will spread over L1 and then the better the encapsulation yield will be. That is the reason why protein precipitates in solvated state have been used for the formulation. In this study, continuous phase is water in which proteins are literally soluble, but it can be envisaged to increase S_3 by using another continuous phase like ethanol, which is not a solvent of proteins, to make greater $\gamma_{L1/L2}$.

3.2. Formulation of lysozyme-loading particles using emulsification/extraction method in CO_2 medium

3.2.1. Protein precipitation using DMI

Activity yield corresponding to experimental points are listed in Table 1. Besides the fact that 100% of protein recovery could be obtained at different conditions of precipitation, the minimum value found at experimental points was 76.7%, which is very promising for the use of DMI to precipitate protein. It can be seen via the

optimal pathway (Fig. 7) the trend of activity yield according to the chosen variables. In fact, when activity yield changed from the minimum value to the maximum one, while other factors stayed almost at the same level, protein quantity changed its sign from positive to negative, which means protein quantity apparently played an important role in this process. Having mentioned that, it needs to be emphasized that yield maximization only occurred when ionic strength and aqueous volume were at a certain level. Therefore, it will be unsurprising if some interactions such as b_{13}, b_{23}, and b_{123} are also found to be significant. The empirical model above-mentioned in Section 2.2.2 was fit to the data for predictive purpose. The model was validated by evaluating the residuals of the check points. Result from Table 2 shows that statistically there are no difference between the residuals and the pure experimental error, which permits the postulated model to be validated. Furthermore, an ANOVA test was performed. It is shown in Table 3 that the chosen model is significant and the overall lack-of-fit is not statistically greater than the pure experimental error. Therefore, the postulated model with its coefficients summarized in Table 4 is suitable for the prediction of activity yield in the chosen ranges of parameters. As already said above, it can be found in this table that not only b_3 but also b_{13}, b_{23}, and b_{123} were significant. To illustrate the equation used for prediction, the activity yield is mapped over the experimental domain at the cut of X_2 = 90 μl in a contour plot and in a 3D surface plot (Fig. 8). Our goal in this formulation part is to prepare protein precipitates whose activity yield is at least 95%. Hence, a desirability function was elaborated with the minimum value set at 95% and the target value set at 100% to help us in finding the region where our goal is satisfied. The result at the cut of X_2 = 90 μl is shown in Fig. 9. The following combination of X_1 = 0.3 M, X_2 = 90 μl, X_3 = 0.9 mg where activity yield was found to be about 95.6 ± 3.2% was chosen for the encapsulation process in CO_2 medium, which is the topic of the next paragraph.

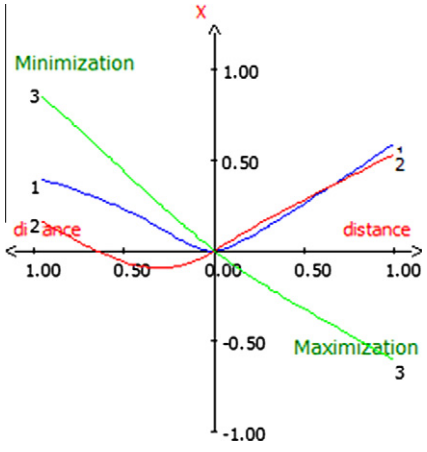

Fig. 7. Optimal pathway of activity yield of lysozyme precipitates prepared using DMI. (For interpretation of the references to color in this figure legend, the reader is referred to the web version of this article.)

Table 2
Validation of empirical model using check points.

Check points	Observed value	Calculated value	Difference	*df*	*p*-value
19	87.50	94.40	−6.90	7	0.141
20	90.00	93.72	−3.72	7	0.400
21	102.50	98.17	4.33	7	0.331
22	94.50	90.67	3.83	7	0.387

Table 3
ANOVA table showing the significance of the model and the lack-of-fit test.

Source	Sum of squares	*df*	Mean square	*F*-value	*p*-value
Model	915.961	10	91.596	5.3867	0.00512**
Residual	187.045	11	17.004		
Lack-of-fit	105.056	6	17.509	1.0678	0.481
Pure error	81.988	5	16.397		
Total	1103.01	21			

** *p*-value < 0.01.

Table 4
Estimation of coefficients in the chosen special cubic model used for prediction of activity yield in the preparation of lysozyme precipitates.

	Coefficient	F. inflation	Std. deviation	*t*. Exp.	*p*-value
b0	95.66		1.44	66.45	<0.0001***
b1	−2.43	1.34	2.30	−1.06	0.3130
b2	5.72	1.00	1.98	2.88	0.0148*
b3	−5.64	1.00	1.98	−2.84	0.0159*
b1-1	−3.65	1.07	3.27	−1.12	0.2880
b2-2	−7.92	1.07	3.27	−2.42	0.0339*
b3-3	−7.60	1.02	3.04	−2.50	0.0296*
b1-2	11.33	1.12	4.73	2.39	0.0356*
b1-3	−15.07	1.12	5.31	−2.84	0.0161*
b2-3	−14.76	1.12	5.31	−2.78	0.0179*
b1-2-3	54.82	1.34	20.17	2.72	0.0200*

* *p*-value < 0.05.
*** *p*-value < 0.001.

3.2.2. Preparation of lysozyme-loading particles

Results are listed in Table 5. It can be seen that encapsulation yield of the first 16 experiments varies from 57.8% to 88.9%. However, the firstly assumed quadratic model (*p*-value = 0.0711) fails to explain the variation of the yield in the chosen experimental domain (Table 6). Besides, in this table, one can also note that special cubic model (*p*-value = 0.0021) and cubic model (*p*-value = 0.0008) are found to well describe the variation of encapsulation yield and do not show a significant lack-of-fit. In this series of 11 distinct experiments, we were fully aware that cubic model used up 10 degree of freedom and thus the lack-of-fit test did not have much meaning. At this stage of experimental design, we did not have enough information to rule out any one of these two regression models. Therefore, five extra points (Table 5, experimental points from standard 17 to standard 21) were added into the design space to test the augmented models. These five points were found using exchange algorithm based on I-optimum criterion in the assumption that the phenomenon would be explained by a cubic model. By doing this, it was ensured that prediction variance in the design space in either case, special cubic or cubic, would have a good quality.

After running the extra points, data were collected and analyzed. Firstly, analysis of sequential model sum of squares has been carried out. This analysis consists of testing the truth of a null hypothesis as follows: H_0: the response is invariant to the presence or absence of the group of terms that has been added to the model. Special cubic model versus quadratic model and cubic model versus special cubic model *F*-tests have been performed. While the *p*-value of the former test is 0.0071, which means the term *ABC* should be included in the regression model, the *p*-value of the latter one is 0.5084, much higher than 0.05, proving that the cubic model is not better than the special cubic one in describing the variation of encapsulation yield in the design space. Therefore, it seems reasonable for us to carry on further analysis with special cubic form as the choice of the regression model.

Partial sum of squares of the model are summarized in an ANOVA table (Table 7). It can be noted that the regression model is significant, and there is no significant lack of fit, which means the special cubic model cannot be rejected in the sense of prediction of the response in the chosen experimental domain. In

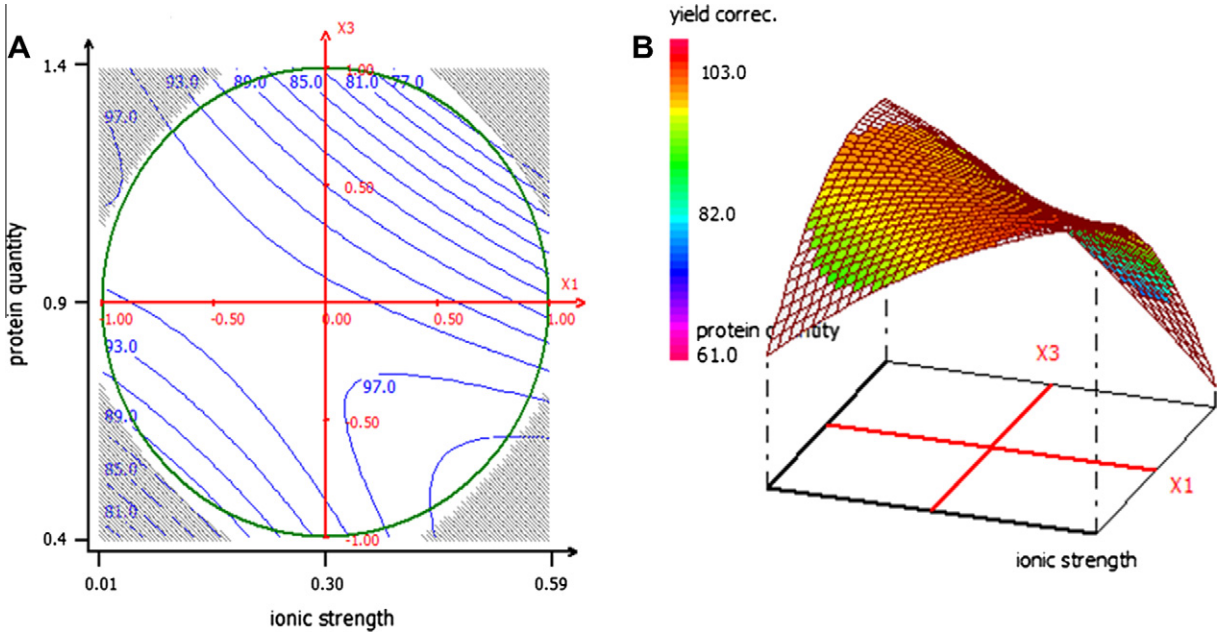

Fig. 8. Activity yield of lysozyme precipitates presented in a contour plot (A) and in a 3D surface (B). Aqueous volume was fixed at 90 μl. (For interpretation of the references to color in this figure legend, the reader is referred to the web version of this article.)

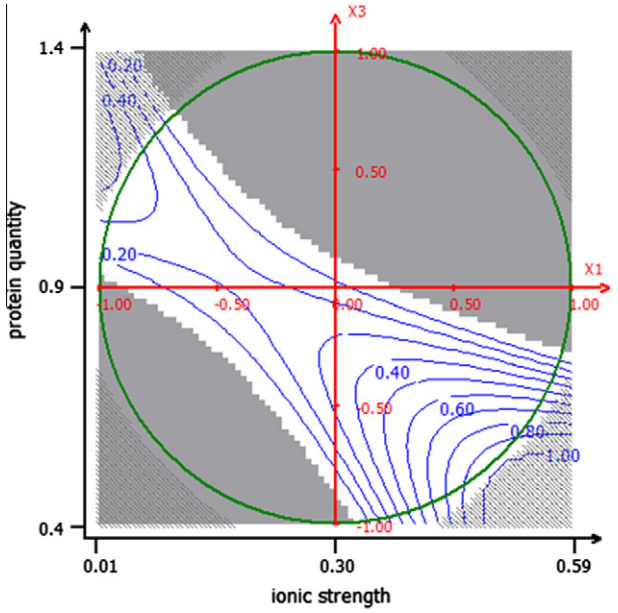

Fig. 9. Contour plot of desirability function. Aqueous volume (X_2) was fixed at 90 μl. (For interpretation of the references to color in this figure legend, the reader is referred to the web version of this article.)

Table 5
Experimental points and the matching encapsulation yield (this experimental design was used for the preparation of lysozyme-loading PLGA particles in CO_2 medium).

Std.	Run	DMI	GF	Ethanol	Yield (%)
1	4	0.544	0.456	0.000	74.4
2	13	1.000	0.000	0.000	60.0
3	7	1.000	0.000	0.000	57.8
4	16	0.843	0.157	0.000	88.9
5	5	0.421	0.500	0.079	65.6
6	14	0.667	0.238	0.095	76.7
7	10	0.667	0.238	0.095	68.9
8	12	0.667	0.238	0.095	73.0
9	3	0.527	0.341	0.131	68.9
10	15	0.819	0.000	0.181	78.9
11	9	0.819	0.000	0.181	77.8
12	1	0.309	0.500	0.191	67.0
13	8	0.309	0.500	0.191	65.4
14	11	0.679	0.087	0.234	85.6
15	2	0.545	0.205	0.250	75.6
16	6	0.405	0.345	0.250	77.5
17	18	0.667	0.333	0.000	75.5
18	21	0.917	0.000	0.083	66.7
19	20	0.750	0.125	0.125	68.9
20	19	0.563	0.250	0.188	76.7
21	17	0.750	0.000	0.250	90.9

Fig. 10B, the response is mapped over the design space in a contour plot and it can be found correspondingly in Fig. 10A the matching standard error of the response expressed in the unit of pure experimental error. The most interesting zone seems to be the orange one in which predicted encapsulation yield can be found from about 85% to 90%. In this zone, ethanol is found to be close to its upper constraint, which is 100 μl. Ethanol, miscible with CO_2 fluid and polymer solution, might decrease interfacial tension between these two phases, thus facilitating the formation of emulsion in CO_2 and then probably allowing a better drug encapsulation. It corroborates with our observation in the view-cell, but it needs to be confirmed by measuring interfacial tension of polymer solution under different conditions of solvent mixture in CO_2 medium. Beyond the scope of this work, it will be the subject of another paper. However, it needs to be emphasized that, based on our previous work in CO_2 medium, the use of ethanol should be limited to a certain level because it might be harmful for protein activity.

Image of PLGA particles observed under scanning electron microscopy (SEM) is shown in Fig. 11C. The particles look spherical and well separated one from the others, which implies that solvents have been successfully extracted. Another indication of it is that the glass transition temperature is about 34 °C, 6.5 °C higher than the one obtained from sample prepared by phase separation method (Table 8). About particle size, it can be noted that average size is smaller in the case of particles prepared by phase separation method than those prepared by emulsification/extraction in CO_2.

Table 6
ANOVA table of different models before the design was augmented.

Source	Sum of squares	*df*	Mean square	*F*-value	*p*-value	Conclusion
ANOVA for Scheffé quadratic model						
Model	646.78	5	129.36	2.91	0.0711	Not significant
Residual	445.23	10	44.52			
Lack of fit	410.48	5	82.10	11.81	0.0085	Significant
ANOVA for Scheffé special cubic model						
Model	937.40	6	156.23	9.09	0.0021	Significant
Residual	154.61	9	17.18			
Lack of fit	119.86	4	29.97	4.31	0.0704	Not significant
ANOVA for Scheffé cubic model						
Model	1057	9	117.44	20.13	0.0008	Significant
Residual	35.01	6	5.83			
Lack of fit	0.25	1	0.25	0.036	0.8561	Not significant
Pure error	34.75	5	6.95			
Corrected total	1092	15				

Table 7
ANOVA table showing the significance of special cubic model and the lack-of-fit test.

Source	Sum of squares	*df*	Mean square	*F*-value	*p*-value	
Model	1203.43	6	200.57	9.86	0.0002	Significant
Linear mixture	283.90	2	141.95	6.98	0.0079	
AB	330.71	1	330.71	16.25	0.0012	
AC	31.23	1	31.23	1.53	0.2358	
BC	4.16	1	4.16	0.20	0.6581	
ABC	202.08	1	202.08	9.93	0.0071	
Residual	284.85	14	20.35			
Lack-of-fit	250.10	9	27.79	4.00	0.0706	Not significant
Pure error	34.75	5	6.95			
Corrected total	1488.29	20				

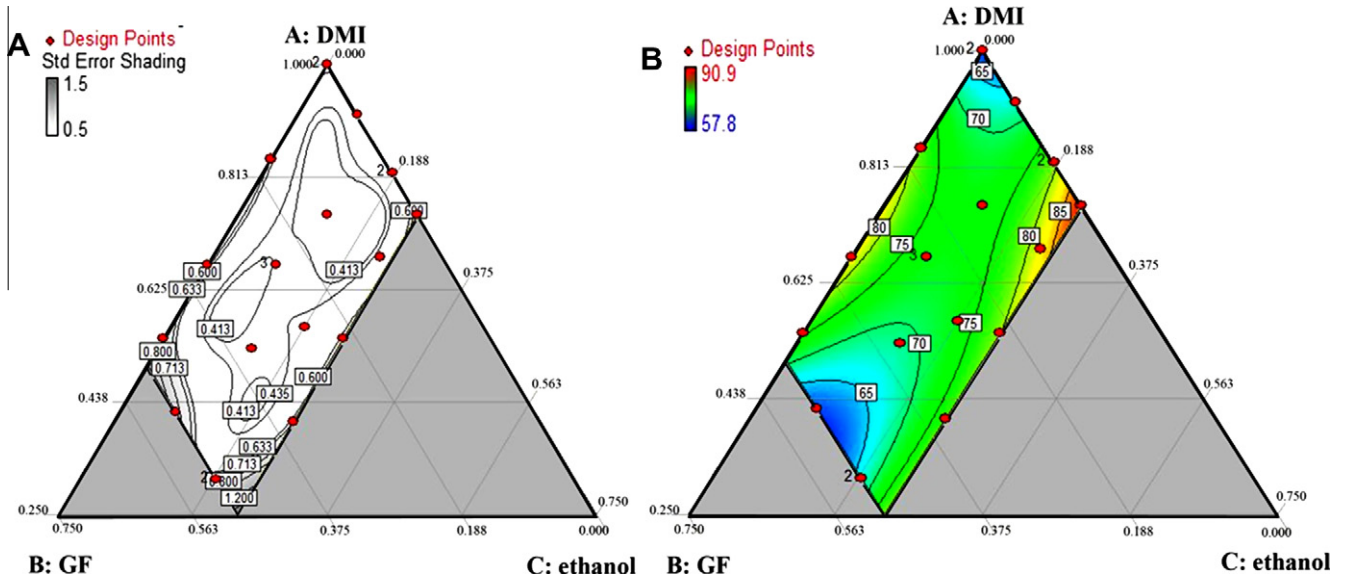

Fig. 10. Predicted activity yield and prediction standard error maps. (A) Contour plot of prediction standard error of special cubic model; (B) contour plot of predicted activity yield. (For interpretation of the references to color in this figure legend, the reader is referred to the web version of this article.)

Table 8
Some characteristics of PLGA particles prepared by phase separation and emulsification/extraction.

Method	Size (nm)		Glass transition temperature (T_g °C)
	Mean	Distribution's standard deviation	
Phase separation	249	51	27.5
Emulsification/extraction[a]	2800	2650	33.9

[a] Analysis was performed with particles prepared under condition of Std. 14 (Table 5).

Moreover, distribution's standard deviation in the case emulsification/extraction is much higher, which is no doubt for us typical of the presence of an emulsification step in the process. Hereby, we present a proof of concept of our process based on an emulsification/extraction method, which theoretically permits particle size to be tuned to suit different applications by modifying the shear stress in emulsification step. Some properties of PLGA particles formulated by the two methods are summarized in Table 8.

Besides, in comparison with the phase separation method, working with solvent mixtures in CO_2 medium gives us more

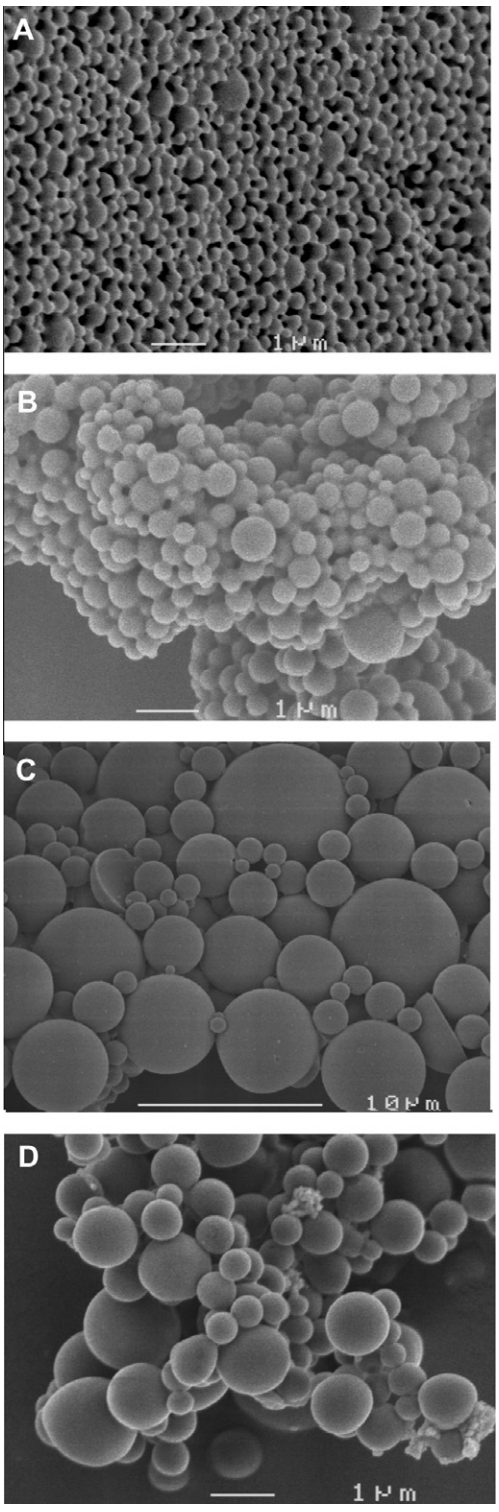

Fig. 11. PLGA particles observed under electron microscopy. (A and B) Particles prepared using phase separation method. In (B) glycine–NaCl buffer, 0.625 M pH 10 was used as the solution Y; (C and D) particles prepared using emulsification/extraction in CO_2 medium. In (D), poly (ε-caprolacton) was mixed with PLGA at a ratio of 1/9 (w/w).

flexibility in the sense of modifying polymer composition or machine configuration to adapt our purpose. For instance, PLGA can be mixed with poly ε-caplactone, which is not soluble in GF and thus cannot be used in phase separation method, to seek a more sustained, or at least a modified release behavior compared to the one produced by pure PLGA [41]. SEM image of particles prepared from a blend of PLGA and poly ε-caprolactone is shown in Fig. 11D.

4. Conclusion

In this paper, we have presented two methods using non-toxic solvents for the preparation of PLGA particles. These methods were used for protein encapsulation purpose but could also be adapted to the encapsulation of other drugs. Each method has its own advantages and also comes with certain disadvantages. Phase separation proves itself as a simple way to generate PLGA particles; however, further effort will be required to fully understand how to modify and to control particle size. Emulsification/extraction in CO_2 offers more options to change the properties of PLGA particles in terms of particle size or polymer composition; however, the indispensable use of a specific machine and CO_2 may be the weak point in this method compared to the phase separation one. Based on the results obtained from this study, it seems reasonable to pursue further steps in the development of these drug carrier systems. Influence of operating parameters on particle size, process robustness, *in vitro* release, and *in vivo* release will be carried out. Besides, working with other types of biodegradable polymers like pegylated-PLGA is also envisaged.

Acknowledgements

The authors thank the financial support of ANR (France—Project ANR-09-PIRI-0004-01), Regional research program (Pays de Loire, France—Bioregos program), and the French education minister. We would like to thank the SCIAM (“Service Commun d’Imagerie et d’Analyse Microscopique”) of Angers for scanning electron microscopy images.

References

[1] J.S. Kent, D.H. Lewis, L.M. Sanders, T.R. Tice, Microencapsulation of Water Soluble Active Polypeptides, Syntex (USA) Inc. (Palo Alto, CA), U.S. Patent 4,675,189, 1987.
[2] F.G. Hutchinson, B.J.A. Furr, Biodegradable carriers for the sustained release of polypeptides, Trends Biotechnol. 5 (1987) 102–106.
[3] V.-T. Tran, J.-P. Karam, X. Garric, J. Coudane, J.-P. Benoît, C.N. Montero-Menei, M.-C. Venier-Julienne, Protein-loaded PLGA–PEG–PLGA microspheres: a tool for cell therapy, Eur. J. Pharm. Sci. 45 (2012) 128–137.
[4] K. Andreas, R. Zehbe, M. Kazubek, K. Grzeschik, N. Sternberg, H. Bäumler, H. Schubert, M. Sittinger, J. Ringe, Biodegradable insulin-loaded PLGA microspheres fabricated by three different emulsification techniques: Investigation for cartilage tissue engineering, Acta Biomater. 7 (2011) 1485–1495.
[5] G.S. Kwon, Improving the stability of PLGA-encapsulated proteins, in: Polymeric Drug Delivery Systems, Taylor & Francis, 2005. pp. 381–416.
[6] A. Aubert-Pouëssel, M.-C. Venier-Julienne, A. Clavreul, M. Sergent, C. Jollivet, C.N. Montero-Menei, E. Garcion, D.C. Bibby, P. Menei, J.-P. Benoit, In vitro study of GDNF release from biodegradable PLGA microspheres, J. Control. Release 95 (2004) 463–475.
[7] T. Morita, Y. Sakamura, Y. Horikiri, T. Suzuki, H. Yoshino, Protein encapsulation into biodegradable microspheres by a novel S/O/W emulsion method using poly(ethylene glycol) as a protein micronization adjuvant, J. Control. Release 69 (2000) 435–444.
[8] C. Thomasin, H.P. Merkle, B.A. Gander, Physico-chemical parameters governing protein microencapsulation into biodegradable polyesters by coacervation, Int. J. Pharm. 147 (1997) 173–186.
[9] J. Kluge, F. Fusaro, N. Casas, M. Mazzotti, G. Muhrer, Production of PLGA micro- and nanocomposites by supercritical fluid extraction of emulsions: I. Encapsulation of lysozyme, J. Supercrit. Fluid 50 (2009) 327–335.
[10] B. Gander, P. Johansen, H. Nam-Trân, H.P. Merkle, Thermodynamic approach to protein microencapsulation into poly(D,L-lactide) by spray drying, Int. J. Pharm. 129 (1996) 51–61.
[11] S.P. Schwendeman, M. Tobío, M. Joworowicz, M.j. Alonso, R. Langer, New strategies for the microencapsulation of tetanus vaccine, J. Microencapsul. 15 (1998) 299–318.
[12] K.G. Carrasquillo, A.M. Stanley, J.C. Aponte-Carro, P. De Jésus, H.R. Costantino, C.J. Bosques, K. Griebenow, Non-aqueous encapsulation of excipient-stabilized spray-freeze dried BSA into poly(lactide-co-glycolide) microspheres results in release of native protein, J. Control. Release 76 (2001) 199–208.

[13] P. Kinam, Y. Yoon, Microencapsulation of protein drugs, in: Tissue Engineering and Novel Delivery Systems, CRC Press, 2003, p. 315.
[14] C. Thomasin, H. Nam-Trân, H.P. Merkle, B. Gander, Drug microencapsulation by PLA/PLGA coacervation in the light of thermodynamics. 1. Overview and theoretical considerations, J. Pharm. Sci. 87 (1998) 259–268.
[15] M.J. Whitaker, J. Hao, O.R. Davies, G. Serhatkulu, S. Stolnik-Trenkic, S.M. Howdle, K.M. Shakesheff, The production of protein-loaded microparticles by supercritical fluid enhanced mixing and spraying, J. Control. Release 101 (2005) 85–92.
[16] A. Hatefi, B. Amsden, Biodegradable injectable in situ forming drug delivery systems, J. Control. Release 80 (2002) 9–28.
[17] H.B. Ravivarapu, K.L. Moyer, R.L. Dunn, Sustained suppression of pituitary-gonadal axis with an injectable, in situ forming implant of leuprolide acetate, J. Pharm. Sci. 89 (2000) 732–741.
[18] U. Bilati, E. Allémann, E. Doelker, Nanoprecipitation versus emulsion-based techniques for the encapsulation of proteins into biodegradable nanoparticles and process-related stability issues, AAPS PharmSciTech 6 (2005) E594–E604.
[19] R.O. Beauchamp Jr., J.W. Ward, B.V. Franko, Dimethylisosorbide Solvent for Muscle Relaxant Drugs, A.H. Robins Company Incorporated (Richmond, VA), U.S. Patent 3,699,230, 1972.
[20] A.R. Bell, F. Cochrane, G.N. O'connor, J.S. Rowe, Formulations for Anaesthetic Use, Parnell Laboratories (Aust) Pty Limited (New South Wales, AU), U.S. Patent 7,326,735, 2008.
[21] J.L. Chen, J.M. Battaglia, Topical and Other Type Pharmaceutical Formulations Containing Isosorbide Carrier, E.R. Squibb & Sons, Inc. (Princeton, NJ), U.S. Patent 4,082,881, 1978.
[22] M. Durr, H.U. Fribolin, E. Harhausen, J. Seidel, Use of Glycofurol for the Liquidization of Pharmaceutical Preparations to be Filled into soft Gelatine Capsules, A. Nattermann & CIE GmbH (Cologne, DE), U.S. Patent 4,842,865, 1989.
[23] L.A. Luzzi, J.K.H. Ma, Dimethyl Isosorbide in Liquid Formulation of Aspirin, Research Corporation (New York, NY), U.S. Patent 4,228,162, 1980.
[24] F. Mottu, A. Laurent, D.A. Rüfenacht, E. Doelker, Organic solvents for pharmaceutical parenterals and embolic liquids: a review of toxicity data, PDA J. Pharm. Sci. Technol. 54 (2000) 456–469.
[25] F. Mottu, M.J. Stelling, D.A. Rüfenacht, E. Doelker, Comparative hemolytic activity of undiluted organic water-miscible solvents for intravenous and intra-arterial injection, PDA J. Pharm. Sci. Technol. 55 (2001) 16–23.
[26] F. Mottu, P. Gailloud, D. Massuelle, D.A. Rüfenacht, E. Doelker, In vitro assessment of new embolic liquids prepared from preformed polymers and water-miscible solvents for aneurysm treatment, Biomaterials 21 (2000) 803–811.
[27] A. Laurent, F. Mottu, R. Chapot, J.Q. Zhang, O. Jordan, D.A. Rüfenacht, E. Doelker, J.J. Merland, Cardiovascular effects of selected water-miscible solvents for pharmaceutical injections and embolization materials: a comparative hemodynamic study using a sheep model, PDA J, Pharm. Sci. Technol. 61 (March–April) (2007) 64–74.
[28] A. Giteau, M.-C. Venier-Julienne, S. Marchal, J.-L. Courthaudon, M. Sergent, C. Montero-Menei, J.-M. Verdier, J.-P. Benoit, Reversible protein precipitation to ensure stability during encapsulation within PLGA microspheres, Eur. J. Pharm. Biopharm. 70 (2008) 127–136.
[29] M.J. Anderson, P.J. Whitcomb, Getting the most from minimal-run designs, in: DOE Simplified: Practical Tools for Effective Experimentation, Taylor and Francis, 2007. pp. 115–132.
[30] NIST/SEMATECH, Mirror-image foldover design, in: e-Handbook of Statistical Methods, 2010. <http://itl.nist.gov/div898/handbook/pri/section3/pri3381.htm>.
[31] G.A. Lewis, D. Mathieu, RogerTan Luu Phan, Response surface methodology, in: Pharmaceutical Experimental Design, Marcel Dekker, New York, 1998. pp. 218–230.
[32] F. Boury, J.P. Benoit, O. Thomas, F. Tewes, Method for Preparing Particles from an Emulsion in Supercritical or Liquid CO_2, Patent WO2007072106, 2005.
[33] J.A. Cornell, The canonical polynomials, in: Experiments with Mixtures: Design, Models, and the Analysis of Mixture Data, John Wiley & Sons, Inc., 2002. pp. 25–30.
[34] W.F. Smith, Designs for non-simplex-shaped region, in: Experimental Design for Formulation, Society for Industrial and Applied Mathematics, 2005, pp. 61–93.
[35] A. Atkinson, A. Donev, R. Tobias, Criteria of optimality, in: Optimum Experimental Designs, with SAS, Oxford Statistical Science Series, Oxford University Press, USA, 2007, pp. 135–150.
[36] L.A. Belfiore, Effect of particle size or film thickness on the glass transition temperature, in: Physical Properties of Macromolecules, John Wiley & Sons, 2010. pp. 31–34.
[37] F. Yuan, M. Dellian, D. Fukumura, M. Leuing, D.A. Berk, V.P. Torchillin, R.K. Jain, Vascular Permeability in a Human Tumor Xenograft: Molecular Size Dependence and Cutoff Size, AACR, Philadelphia, United States, 1995.
[38] H. Hashizume, P. Baluk, S. Morikawa, J.W. McLean, G. Thurston, S. Roberge, R.K. Jain, D.M. McDonald, Openings between defective endothelial cells explain tumor vessel leakiness, Am. J. Pathol. 156 (2000) 1363–1380.
[39] S.K. Hobbs, W.L. Monsky, F. Yuan, W.G. Roberts, L. Griffith, V.P. Torchilin, R.K. Jain, Regulation of transport pathways in tumor vessels: role of tumor type and microenvironment, Proc. Natl. Acad. Sci. USA 95 (1998) 4607–4612.
[40] J.H. Park, S. Lee, J.-H. Kim, K. Park, K. Kim, I.C. Kwon, Polymeric nanomedicine for cancer therapy, Prog. Polym. Sci. 33 (2008) 113–137.
[41] R.C. Mundargi, S. Srirangarajan, S.A. Agnihotri, S.A. Patil, S. Ravindra, S.B. Setty, T.M. Aminabhavi, Development and evaluation of novel biodegradable microspheres based on poly(D,L-lactide-co-glycolide) and poly(ε-caprolactone) for controlled delivery of doxycycline in the treatment of human periodontal pocket: in vitro and in vivo studies, J. Control. Release 119 (2007) 59–68.